

The Electrochemical Behavior of Gold-Silver Alloy Nanoparticles

Blake J. Plowman,^[a] Boopathi Sidhureddy,^[b] Stanislav V. Sokolov,^[a] Neil P. Young,^[c] Aicheng Chen^[b] and Richard G. Compton^{*[a]}

Abstract: We report the voltammetry of alloy nanoparticles via the cyclic voltammetry of gold-silver alloy nanoparticles. Through careful comparison with the response of pure gold nanoparticles, pure silver nanoparticles and their mixture the contrasting electrochemical behavior of the alloy nanoparticles is established, providing insights into the electrochemical stability of gold-silver alloy nanoparticles in chloride-containing media.

The design, fabrication and characterization of nanoparticles is a major research theme, driven by the fascinating behavior of nanoparticles as compared with bulk materials, along with the desire to tailor their properties towards a wide range of applications. Often this is accomplished by altering the size, shape and chemical functionalization of the nanomaterials, however it has also been identified that the properties may be readily controlled by altering their composition.^[1] This has extended from the use of a wide variety of monometallic nanoparticles (including gold, silver, copper and platinum to name a few) to the use of bimetallic nanoparticles, where such nanomaterials may take the form of alloy,^[2] or core-shell^[3] or Janus structures.^[4] Alloy nanoparticles have proven especially interesting from an applied point of view, as the well-ordered structures can provide altered catalytic, magnetic and optical properties.^[2, 5] However while much attention has been directed towards the synthesis of such structures, an important feature in this field is the stability of the materials under operating conditions. This is necessitated as it is known that alloy nanoparticles can be prone to undergo phase separation or dealloying, which will in turn result in altered and potentially unwanted changes in activity.^[6] This is especially true for electrochemical systems such as sensors or electrocatalytic arrays, where the influence of the applied potential in the presence of a range of supporting electrolytes may promote modifications in the structure of the nanoparticles, thereby leading to suboptimal performance.

In this work we explore the voltammetric behavior of gold-silver alloy nanoparticles in a chloride containing environment. We are motivated to study the electrochemical behavior of alloy nanoparticles, given the interest in gold-silver alloy nanoparticles for use in catalysis,^[7] electrocatalysis,^[8] sensing,^[9] luminescence,^[10] and biological applications.^[11] As such this presents a model system to probe the electrochemical stability

of alloy nanoparticles.

Following the synthesis of the gold-silver alloy nanoparticles (as outlined in the Experimental Section) the structure of the nanoparticles was screened by UV-visible spectroscopy. As is shown in Figure 1, spherical citrate-capped gold (blue curve) and silver (black curve) nanoparticles displayed surface plasmon resonance (SPR) peaks at 536 nm and 421 nm, respectively, in agreement with prior work.^[12] For the case of the gold-silver nanoparticles a single SPR peak was observed at 472 nm. The position of this peak is in excellent agreement with the linear relationship expected between the SPR peak position and the composition of the bimetallic nanoparticles (Figure 1 Inset).^[13] Also of note is the absence of any peaks at the wavelengths where the gold and silver nanoparticles displayed maxima, indicating that the nanoparticles formed are indeed gold-silver alloy nanoparticles, as the presence of monometallic nanoparticles would lead to the appearance of additional peaks in the UV-visible spectrum.^[14]

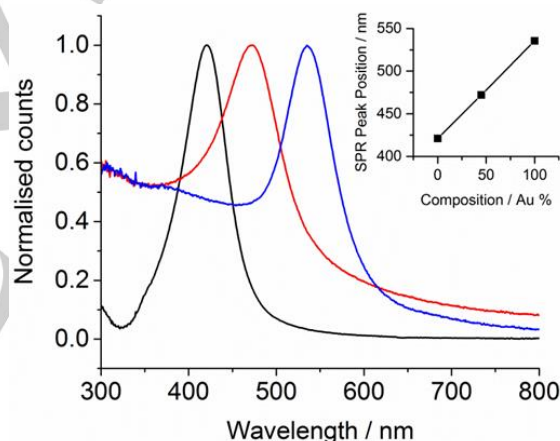


Figure 1. UV-visible spectroscopy for aqueous silver (black), gold-silver (red) and gold (blue) nanoparticle suspensions, with the composition dependent SPR peak positions shown in the inset.

The morphology of the nanoparticles was next investigated by transmission electron microscopy (TEM). As seen in Figure 2a the particles were found to be quasi-spherical in nature. A total of 300 nanoparticles were sized (Figure 2b), from which the modal nanoparticle size was determined to be 50.5 nm. Interestingly it has been noted that the formation of gold-silver alloy nanoparticles with diameters greater than 30 nm is difficult to achieve, and indeed efforts such as the growth of alloys on seed nanoparticles have been reported to overcome this issue.^[15] However in the present work the co-reduction of HAuCl_4 and AgNO_3 in the presence of citrate was found to produce relatively large gold-silver alloy nanoparticles without the requirement of seed nanoparticles, simplifying the synthesis procedure and avoiding the formation of a core-shell type morphology.

[a] Dr. Blake J. Plowman, Stanislav V. Sokolov, Prof. Richard G. Compton
Physical and Theoretical Chemistry Laboratory
Department of Chemistry, University of Oxford
South Parks Road, Oxford, OX13QZ, UK
E-mail: richard.compton@chem.ox.ac.uk

[b] Dr. Boopathi Sidhureddy, Prof. Aicheng Chen
Department of Chemistry, Lakehead University
955 Oliver Road, Thunder Bay, ON P7B 5E1, Canada

[c] Dr. Neil P. Young
Department of Materials, University of Oxford
Parks Road, Oxford, OX13PH, UK

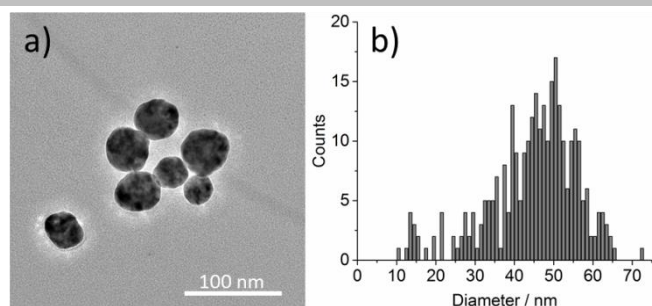


Figure 2. a) Bright field TEM image of gold-silver alloy nanoparticles, with the size distribution of the particles given in b).

The composition and structure of the nanoparticles was then further investigated by TEM. Presented in Figure 3a is an image of a gold-silver nanoparticle taken using high angle annular dark field scanning transmission electron microscopy (HAADF-STEM) mode. Here a quasi-spherical nanoparticle can be seen, showing a small protrusion at the top of the nanoparticle. From the bright field imaging of similar nanoparticles (Figure S1) it can be seen that these features are extremely thin and may indicate a partial rearrangement of the nanoparticle surface. Also of note from this image is the even contrast present across the particle. Due to the higher atomic number contrast achieved by HAADF-STEM imaging compared with bright field imaging^[16] this method has previously been used to image the homogeneity of gold and silver distributions,^[17] evidencing that in the present case the sample is comprised of well alloyed nanoparticles. Confirmation of this was obtained by energy dispersive X-ray (EDX) mapping, where the distributions of silver (Figure 3b) and gold (Figure 3c) are shown to be even across the nanoparticles, as is seen in the overlaid gold and silver map in Figure 3d. Interestingly the small protrusion at the top of the nanoparticle can be readily identified as a small region of silver, given that this feature is present in the silver map but absent in the gold map (Figure 3c). The finding that the alloy nanoparticles are well ordered is in agreement with the UV-visible spectroscopy results shown in Figure 1, demonstrating the success of the synthesis procedure.

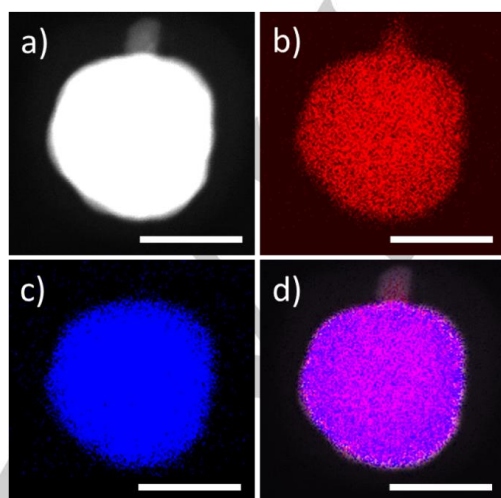
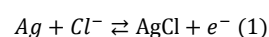
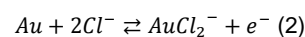


Figure 3. Dark field TEM image of a gold-silver nanoparticle (a) with the corresponding EDX maps for silver (b), gold (c) and the combined gold and silver map (d).

After establishing the structure of the nanoparticles, voltammetry was then performed in KCl to investigate the electrochemical behavior of the alloy nanoparticles in a chloride-containing electrolyte, as may be readily encountered in electrocatalytic or sensing applications. First the voltammetry of the monometallic nanoparticles was studied, with the response of a silver nanoparticle modified glassy carbon electrode shown in Figure 4a. Here a large oxidative peak is observed in the first scan (red curve) at 0.15 V. This is in agreement with prior work and is due to the oxidation of silver to silver chloride, as is given by Equation 1.^[18] No further peaks are observed in the forward scan, and on the reverse scan only traces of silver chloride reduction can be seen at potentials below 0 V. Similar features are present for the second scan (black curve), although the magnitude of the silver oxidation peak is greatly diminished (8.3 μC for the first scan and 0.3 μC for the second scan). As this decrease could be related to either the loss of silver from the surface or the incomplete reduction of silver chloride in the first scan, voltammetry was also performed with a lower potential limit (Figure S2). Here the reduction of AgCl on glassy carbon can be clearly identified below 0 V, and upon cycling the silver oxidation peak remains of at a comparable magnitude with the first scan. From this result the diminished silver oxidation peak for the second scan in Figure 4c is therefore attributed to the incomplete reduction of the silver chloride which formed in the first scan.



The cyclic voltammetry of the gold nanoparticles was next performed, and as can be seen from Figure 4b an oxidative process is observed at 1.04 V in the first scan (red curve). This feature, in combination with the diminished response in the second scan is attributed to the oxidative dissolution of gold in the presence of Cl^- , which has previously been demonstrated to occur via the formation of both Au(I) and Au(III) chlorides (Equations 2 and 3, respectively).^[19]



Having investigated the electrochemical behaviour of the gold and silver nanoparticles separately, voltammetry was then performed for a glassy carbon surface modified with both pure gold and pure silver nanoparticles together. As is shown in Figure 4c, this resulted in the appearance of a sharp oxidation peak at 0.14 V, in close agreement with the silver oxidation observed in Figure 4a. At higher potentials gold oxidation can also be seen, with an oxidation peak apparent at 1.02 V, as was seen in Figure 4b. However, unlike in the case of the monometallic nanoparticles alone in the reverse scan a reduction peak is readily seen at 0.01 V, which is attributed to the reduction of silver chloride formed in the forward scan.^[18, 20] As it is known that upon drop casting on an electrode surface nanoparticle agglomeration can take place,^[21] in the present case this will result in the adjacency of the gold and silver nanoparticles. As such the gold nanoparticles may act as nucleation sites which facilitate the reduction of silver chloride at less negative potentials than are required for the glassy carbon electrode alone (Figure S2). Interestingly on the second scan the magnitude of the silver oxidation peak is comparable with the first scan, a finding not observed for the silver nanoparticles within this potential region (Figure 4a). This provides further evidence that the decreased silver oxidation for the latter sample

is the result of the incomplete reduction of silver chloride, which is overcome by the addition of gold nanoparticles.

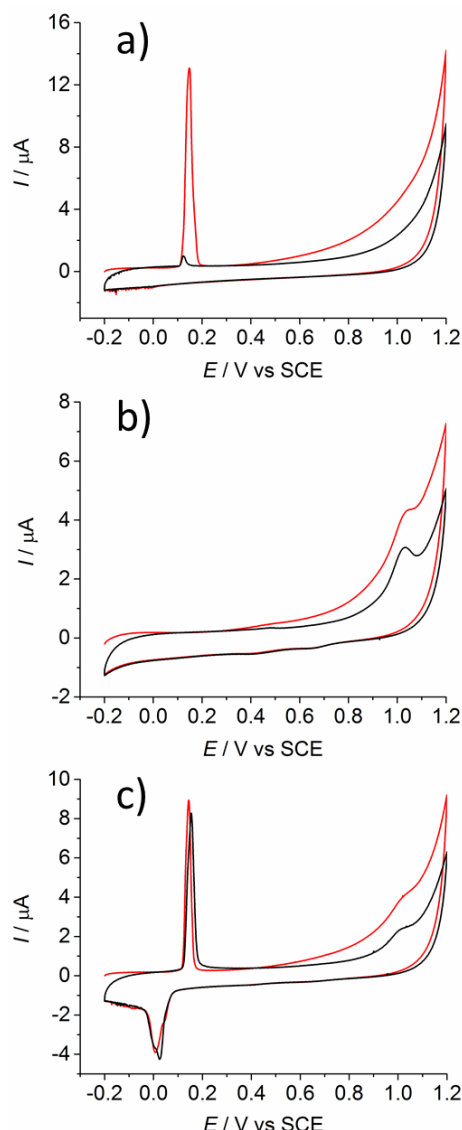


Figure 4. Cyclic voltammograms recorded in 20 mM KCl at 50 mV s⁻¹ showing the first (red) and second (black) scans for glassy carbon electrodes modified with 4 μL of 15 pM silver nanoparticles (a), 15 pM gold nanoparticles (b) and 7.5 pM gold nanoparticles with 7.5 pM silver nanoparticles (c).

After establishing the voltammetric responses of gold and silver nanoparticles, along with their mixture, the voltammetry of the gold-silver alloy nanoparticles was then investigated. As is shown in Figure 5 the first cycle (red curve) presents significantly altered behaviour in comparison with the monometallic samples. Small oxidation peaks are present at 0.11 V and 0.13 V, while the major oxidation peak in the silver region is found at 0.31 V. This latter oxidative feature is found to be 160 mV more positive compared with the oxidation peak for the silver nanoparticles (Figure 4a). Due to the comparable nanoparticle sizes for the silver nanoparticles and the alloy nanoparticles the shifted oxidation potential is not attributed to a size effect but rather to the oxidation of silver which is stabilized by the alloy matrix with the gold component.^[22] Interestingly the

small oxidation peaks present in this scan occur at a similar potential to the oxidation potential of the silver nanoparticles and are therefore attributed to the oxidation of small silver-only features on the alloy nanoparticles, which is in excellent agreement with the silver protrusions identified by EDX mapping (Figure 3). At more positive potentials a further oxidation peak is apparent (0.98 V), evidencing the oxidative dissolution of gold. Upon reversing the scan a sharp reduction peak is present at 0.03 V, showing that as with the mixed gold and silver nanoparticle sample the alloy nanoparticles provide suitable nucleation points to drive the reduction of silver chloride at higher potentials. This finding was also observed when the upper potential limit was reduced to 0.6 V (Figure S3) showing that gold oxidation products are not involved.

Upon the second cycle (black curve) the silver oxidation peak observed at 0.31 V is no longer present, and the small silver oxidation peaks at 0.11 V and 0.13 V are replaced by a large oxidation peak at 0.16 V. In contrast the gold oxidation peak at 0.98 V is seen to decrease in the second scan, while the magnitude of the reductive peak at 0.03 V remains constant. These results indicate that in the first scan the oxidation of the small silver-only domains is followed by the oxidation of silver from the alloy, a process which is limited by the availability of silver. Gold oxidation then follows at higher potentials, and as seen by the peak decrease between the first and second scans this dissolution of gold facilitates silver oxidation, resulting in a large silver chloride reduction peak on the reverse scan. This increased silver availability is further seen by the higher amount of silver oxidation in the second scan as compared with the first scan. Importantly on the second scan the presence of the silver oxidation peak at 0.16 V rather than 0.31 V indicates that the cycling has led to the partial dealloying of the nanoparticles, with the silver oxidation now closely resembling the oxidation of pure silver nanoparticles (Figure 4a). These results illustrate that significant restructuring of the alloy nanoparticles occurs under these conditions. This is a significant finding, demonstrating that the structure and therefore the properties of the gold-silver alloys are extremely sensitive towards oxidation.

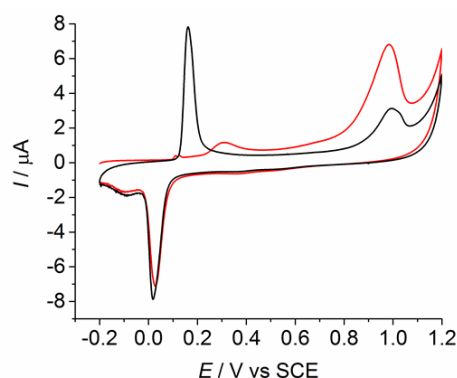


Figure 5. Cyclic voltammograms recorded in 20 mM KCl at 50 mV s⁻¹ showing the first (red) and second (black) scans for a glassy carbon electrode modified with 4 μL of gold-silver alloy nanoparticles.

In this work we have demonstrated the analysis of the electrochemical behavior of gold-silver alloy nanoparticles in

chloride containing media. Such results clearly illustrate the extent of reconfiguration which is undergone by the particles, with the oxidation of silver to silver chloride rapidly changing the response of the particles from that of an alloy to that of a sample containing isolated silver and gold domains. These findings are of importance for potential applications of gold-silver alloys in the presence of chloride, as may be commonly encountered in electrochemical sensing or electrocatalytic platforms, and highlight the importance of testing the stability of alloy nanoparticles in electrochemical systems.

Experimental Section

All solutions were prepared using MilliQ water (Resistivity of 18.2 MΩ cm at 25 °C), with chemicals used as received from Sigma-Aldrich (tetrachloroauric acid, silver nitrate, trisodium citrate, and potassium chloride), Nanopartz (citrate-capped gold nanoparticles, 62.8 ± 4.4 nm) and Nanocomposix (citrate-capped silver nanoparticles, 43.2 ± 3.6 nm). Gold-silver alloy nanoparticles were synthesised by mixing 0.3 mL of 10 mM AgNO₃ and 0.3 mL of 10 mM HAuCl₄ into 23 mL of water. After the solution was boiled, 1.4 mL of 1 % trisodium citrate solution was added. The mixture was continuously boiled under reflux conditions for 10 minutes and then left to cool to air temperature. The formed gold-silver alloy nanoparticles were then stored as a stock suspension.

Nanoparticle characterization was performed TEM using a JEOL JEM-3000F equipped with an energy dispersive X-ray (EDX) spectrometer with an accelerating voltage of 300 kV. Sample preparation involved drop casting nanoparticle suspensions on holey carbon grids (Agar Scientific) and allowing to dry. UV-visible spectroscopy was performed using a UV-1800 Shimadzu spectrometer. Electrochemical experiments were performed at 25 ± 0.2 °C with solutions degassed by nitrogen bubbling, using a µAutolab II potentiostat (Metrohm). A three electrode configuration was utilised with a platinum counter electrode, Kapton tape modified glassy carbon (HTW, 4 mm diameter) working electrodes and a saturated calomel reference electrode (SCE). All potentials quoted in this work are given using this reference electrode.

Acknowledgements

The authors gratefully acknowledge the support of this work through a Marie Curie International Incoming Fellowship (BJP, Project 630069).

Keywords: Alloy • Bimetallic • Electrochemistry • Gold-silver • Nanoparticles

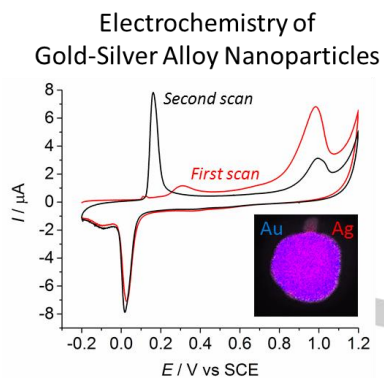
- [1] a) A. R. Tao, S. Habas, P. Yang, *Small* **2008**, *4*, 310-325; b) B. R. Cuenya, *Thin Solid Films* **2010**, *518*, 3127-3150; c) A. Albanese, P. S. Tang, W. C. W. Chan, *Annu. Rev. Biomed. Eng.* **2012**, *14*, 1-16; d) L. Rassaei, F. Marken, M. Sillanpää, M. Amiri, C. M. Cirtiu, M. Sillanpää, *TRAC Trends Anal. Chem.* **2011**, *30*, 1704-1715; e) M. A. O'Connell, J. R. Lewis, A. J. Wain, *Chem. Commun.* **2015**, *51*, 10314-10317.
- [2] R. Ferrando, J. Jellinek, R. L. Johnston, *Chem. Rev.* **2008**, *108*, 845-910.
- [3] a) R. Ghosh Chaudhuri, S. Paria, *Chem. Rev.* **2012**, *112*, 2373-2433; b) C. E. Blackmore, N. V. Rees, R. E. Palmer, *Phys. Chem. Chem. Phys.* **2015**, *17*, 28005-28009.
- [4] G. Zhao, M. Pumera, *Nanoscale* **2014**, *6*, 11177-11180.
- [5] a) Z. Peng, H. Yang, *Nano Today* **2009**, *4*, 143-164; b) C. Gong, M. S. Leite, *ACS Photonics* **2016**.
- [6] a) J. A. Gilbert, A. J. Kropf, N. N. Kariuki, S. DeCrane, X. Wang, S. Rasouli, K. Yu, P. J. Ferreira, D. Morgan, D. J. Myers, *J. Electrochem. Soc.* **2015**, *162*, F1487-F1497; b) C. Cui, L. Gan, M. Heggen, S. Rudi, P. Strasser, *Nat. Mater.* **2013**, *12*, 765-771.
- [7] a) K. S. Shin, J. H. Kim, I. H. Kim, K. Kim, *J. Nanopart. Res.* **2012**, *14*, 1-10; b) G. Nagy, T. Benkő, L. Borkó, T. Csay, A. Horváth, K. Frey, A. Beck, *Reac. Kinet. Mech. Cat.* **2015**, *115*, 45-65.
- [8] a) M. Tominaga, T. Shimazoe, M. Nagashima, H. Kusuda, A. Kubo, Y. Kuwahara, I. Taniguchi, *J. Electroanal. Chem.* **2006**, *590*, 37-46; b) P. Hu, Y. Song, L. Chen, S. Chen, *Nanoscale* **2015**, *7*, 9627-9636; c) A. Pearson, A. P. O'Mullane, S. K. Bhargava, V. Bansal, *Electrochem. Commun.* **2012**, *25*, 87-90.
- [9] a) Latif-ur-Rahman, A. Shah, S. B. Khan, A. M. Asiri, H. Hussain, C. Han, R. Qureshi, M. N. Ashiq, M. A. Zia, M. Ishaq, H.-B. Kraatz, *J. Appl. Electrochem.* **2015**, *45*, 463-472; b) S. N. Mailu, T. T. Waryo, P. M. Ndangili, F. R. Ngece, A. A. Baleg, P. G. Baker, E. I. Iwuoha, *Sensors* **2010**, *10*, 9449; c) M. P. Navas, R. K. Soni, *Appl. Phys. A* **2014**, *116*, 879-886.
- [10] a) K. S. Abhijith, R. Sharma, R. Ranjan, M. S. Thakur, *Photochem. Photobiol. Sci.* **2014**, *13*, 986-991; b) S. Li, S. Tao, F. Wang, J. Hong, X. Wei, *Microchim. Acta* **2010**, *169*, 73-78.
- [11] a) M. M. Santos, M. J. Queiroz, P. V. Baptista, *J. Nanopart. Res.* **2012**, *14*, 1-8; b) S. Patskovsky, E. Bergeron, D. Rioux, M. Simard, M. Meunier, *Analyst* **2014**, *139*, 5247-5253.
- [12] a) W. Haiss, N. T. K. Thanh, J. Aveyard, D. G. Fernig, *Anal. Chem.* **2007**, *79*, 4215-4221; b) S. Agnihotri, S. Mukherji, S. Mukherji, *RSC Adv.* **2014**, *4*, 3974-3983.
- [13] a) S. Link, Z. L. Wang, M. A. El-Sayed, *J. Phys. Chem. B* **1999**, *103*, 3529-3533; b) J. W. L. Eccles, U. Bangert, M. Bromfield, P. Christian, A. J. Harvey, *J. Appl. Phys.* **2010**, *107*, 104325; c) A. Pal, S. Shah, V. Kulkarni, R. S. R. Murthy, S. Devi, *Mater. Chem. Phys.* **2009**, *113*, 276-282.
- [14] M. P. Mallin, C. J. Murphy, *Nano Lett.* **2002**, *2*, 1235-1237.
- [15] D. Rioux, M. Meunier, *J. Phys. Chem. C* **2015**, *119*, 13160-13168.
- [16] S. I. Sanchez, M. W. Small, J.-M. Zuo, R. G. Nuzzo, *J. Am. Chem. Soc.* **2009**, *131*, 8683-8689.
- [17] L. R. Holt, B. J. Plowman, N. P. Young, K. Tschulik, R. G. Compton, *Angew. Chem. Int. Ed.* **2016**, *55*, 397-400.
- [18] E. J. E. Stuart, K. Tschulik, D. Lowinsohn, J. T. Cullen, R. G. Compton, *Sens. Actuators B* **2014**, *195*, 223-229.
- [19] Y.-G. Zhou, N. V. Rees, J. Pillay, R. Tshikhudo, S. Vilakazi, R. G. Compton, *Chem. Commun.* **2012**, *48*, 224-226.
- [20] R. Hao, Y. Fan, B. Zhang, *J. Electrochem. Soc.* **2016**, *163*, H3145-H3151.
- [21] a) H. S. Toh, C. Batchelor-McAuley, K. Tschulik, M. Uhlemann, A. Crossley, R. G. Compton, *Nanoscale* **2013**, *5*, 4884-4893; b) K. Tschulik, C. Batchelor-McAuley, H.-S. Toh, E. J. E. Stuart, R. G. Compton, *Phys. Chem. Chem. Phys.* **2014**, *16*, 616-623.
- [22] a) X. Li, Q. Chen, I. McCue, J. Snyder, P. Crozier, J. Erlebacher, K. Sieradzki, *Nano Lett.* **2014**, *14*, 2569-2577; b) C. A. Starr, D. A. Buttry, *ECS Trans.* **2014**, *58*, 19-26; c) A. Dursun, D. Pugh, S. Corcoran, *J. Electrochem. Soc.* **2003**, *150*, B355-B360.

Entry for the Table of Contents

Layout 1:

COMMUNICATION

The electrochemistry of alloy nanoparticles: Gold-silver alloy nanoparticles are investigated in chloride containing media. Significantly altered electrochemical behaviour is seen relative to pure gold and pure silver nanoparticles, and restructuring of the alloy nanoparticles evident on cycling.



Blake J. Plowman, Boopathi Sidhureddy, Stanislav V. Sokolov, Neil P. Young, Aicheng Chen and Richard G. Compton*

Page No. – Page No.

The Electrochemical Behavior of Gold-Silver Alloy Nanoparticles